ACS AuthorChoice

Environmental Science & Technology

Article

pubs.acs.org/est

Terms of Use

Interactions of Aqueous Ag^+ with Fulvic Acids: Mechanisms of Silver Nanoparticle Formation and Investigation of Stability

Nathaniel F. Adegboyega,[†] Virender K. Sharma,*[,†] Karolina Siskova,[‡] Radek Zbořil,[‡] Mary Sohn,[†] Brian J. Schultz,[§] and Sarbajit Banerjee[§]

[†]Chemistry Department, Florida Institute of Technology, 150 West University Boulevard, Melbourne, Florida 32901, United States

[‡]Regional Centre of Advanced Technologies and Materials, Department of Physical Chemistry, Faculty of Science, Palacky University, Slechtitelu 11, 78371 Olomouc, Czech Republic

[§]Department of Chemistry, 410 Natural Sciences Complex, University at Buffalo The State University of New York, Buffalo, New York 14260, United States

Supporting Information

ABSTRACT: This study investigated the possible natural formation of silver nanoparticles (AgNPs) in Ag^+–fulvic acid (FA) solutions under various environmentally relevant conditions (temperature, pH, and UV light). Increase in temperature (24–90 °C) and pH (6.1–9.0) of Ag^+–Suwannee River fulvic acid (SRFA) solutions accelerated the appearance of the characteristic surface plasmon resonance (SPR) of AgNPs. The rate of AgNP formation via reduction of Ag^+ in the presence of different FAs (SRFA, Pahokee Peat fulvic acid, PPFA, Nordic lake fulvic acid, NLFA) and Suwannee River humic acid (SRHA) followed the order NLFA > SRHA > PPFA > SRFA. This order was found to be related to the free radical content of the acids, which was consistent with the proposed mechanism. The same order of AgNP growth was seen upon UV light illumination of Ag^+–FA and Ag^+–HA mixtures in moderately hard reconstituted water (MHRW). Stability studies of AgNPs, formed from the interactions of Ag^+–SRFA, over a period of several months showed that these AgNPs were highly stable with SPR peak reductions of only ~15%. Transmission electron microscopy (TEM) and dynamic light scattering (DLS) measurements revealed bimodal particle size distributions of aged AgNPs. The stable AgNPs formed through the reduction of Ag^+ by fulvic and humic acid fractions of natural organic matter in the environment may be transported over significant distances and might also influence the overall bioavailability and ecotoxicity of AgNPs.

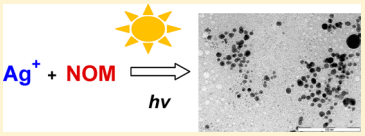

INTRODUCTION

Nanomaterials have been used to modify numerous medical and industrial products such as pharmaceuticals, cosmetics, textiles, paints, surface coatings, electronic components, and additives in food packaging.[1,2] More than 50% of nanomaterials used industrially contain nanoparticulate silver, with an estimated global production of silver nanoparticles (AgNPs) of ~320 000 tons/year.[3] Silver nanoparticles possess antiviral and antibacterial properties, which has inspired numerous applications directed at mitigating bacterial and viral contamination.[4,5] The widespread use of AgNPs is of concern because of potential risks to ecosystems. These risks include direct impacts on microbial communities and subsequent effects on food chains.[6−8] Once AgNPs are released into the aquatic environment, their fate, transport, and bioavailability depend on several properties such as size, surface charge, and nature of their coating groups.[9−11] The mobility and aggregation of AgNPs are influenced by the pH, ionic strength, and individual ionic components of natural waters.[12−14] Recently, the effects of natural organic matter on the stability of engineered AgNPs in the aqueous phase were investigated.[7,15,16] Comparatively, little information is available on the natural formation of AgNPs, or their stability under environmental conditions. Indeed, stable AgNPs could persist in the environment and could be transported over significant distances.

Over the past few years, we have initiated studies on the formation of AgNPs from the reduction of silver ions (Ag^+) by fractions of naturally occurring organic matter.[17] Silver ions are released from industrial effluents related to mining and photographic development and ultimately from municipal water treatment plants.[18−20] Upon entering the environment, silver ions may be transformed into AgNPs by natural reductants such as the functional groups found in organic matter.[17] The presence of colloidal silver in coastal regions was reported in the mid 1990s, which was before the widespread use of AgNPs in consumer products;[21] more recently, substantial silver contamination has been detected in the mining effluents of less developed regions where again the use of products containing AgNPs is less likely.[22] Such occurrences of colloidal silver may be due to the reduction of Ag^+ by fractions of natural organic matter.

Received: June 8, 2012
Revised: November 23, 2012
Accepted: December 13, 2012
Published: December 13, 2012

The primary objective of the present article is to derive insight into the possible natural formation of AgNPs; and more specifically, to explore the influence of pH and UV light on the interaction of hydrated Ag^+ and organic matter resulting in the formation of AgNPs, which has not been previously reported. We have chosen fulvic acids (FAs) as organic matter to demonstrate the formation and stability of AgNPs under environmentally relevant conditions. There is only one previous report in the literature on the reduction of Ag^+ by fulvic acid. In that instance, a peat-derived FA at a concentration of 500 mg L^{-1} and at elevated temperatures (70−90 °C) yielded AgNPs, whose nanoscale dimensions were surmised solely based on observation of a putative plasmon resonance by UV−vis spectroscopy.[23] The objective of that study was to attempt the preparation of bactericidal AgNPs for medical applications without any mention of environmental relevance. The aims of the present study are to (i) determine the effects of temperature and pH on the formation of AgNPs in Ag^+−FA solutions; (ii) study FAs of different origins and compare their relative rates of AgNP formation with those formed in Ag^+−HA solutions; (iii) determine whether UV light can enhance the formation of AgNPs in solutions containing Ag^+ and FAs; (iv) assess the potential role of FAs in the environmental formation and migration of AgNPs.

EXPERIMENTAL SECTION

Chemicals. Silver nitrate (>99.0% purity) was obtained from Sigma Aldrich (St. Louis, MO) and no further purification was performed before experimental use. All fulvic and humic acids were purchased from the International Humic Substances Society (IHSS, St. Paul, MN) and were from aquatic sources with the exception of Pahokee Peat fulvic acid. These acids were designated as SRFA, PPFA, NLFA, and SRHA for Suwannee River fulvic acid I, Pahokee Peat fulvic acid II, Nordic lake fulvic acid, and Suwannee River humic acid II, respectively. Sodium hydrogen phosphate (Na_2HPO_4) and sodium borate ($Na_2B_4O_7{\cdot}10H_2O$) were obtained from Fisher Scientific. All solutions were prepared with water that had been distilled and passed through an 18 MΩ/cm Milli-Q cm water purification system. All glassware was acid washed and soaked in distilled water for ∼12 h prior to use. Standard solutions of FA and HA were prepared in 0.001 M borate and 0.005 M phosphate buffer solution at pH 9.0. In forming the solutions of FA and HA, solids were allowed to dissolve for several hours; after there was visible evidence of their dissolution, solutions were filtered through 0.45-μm filters which had been previously dried and weighed. There was no significant difference in the weight of the dried filtered paper before and after filtration of solutions of FAs and HA. Studies were carried out in the buffer solution and the desired pH was obtained by the addition of phosphoric acid or sodium hydroxide. The pH of the solutions was measured on an Orion pH/ISE meter, model 710A (Thermo Fisher Scientific, Waltham, MA). EPA MHRW (moderately hard reconstituted water) was used as a synthetic freshwater, and was prepared by adding sodium, magnesium, and calcium, chloride, sulfate, and carbonate ions to Milli-Q water to obtain a final pH of 7.8.[24]

Formation of Silver Nanoparticles. AgNPs were formed by reducing silver ions with FA and HA, similar to a previously reported procedure.[17] Briefly, 3 mL of silver nitrate was mixed with 3 mL of FA or HA in a capped test tube under normal laboratory conditions, including exposure to laboratory light. The mixture was stirred for a period ranging from hours to days, depending on the temperature. The reaction temperatures studied were RT (24 ± 1 °C) and 90 ± 1 °C. The formation of AgNPs was monitored at regular intervals by UV−vis spectroscopy. The complete dissolution of FA and HA in buffer solution was confirmed by spectroscopic measurements. Formation of AgNPs was usually monitored until an absorbance value of ∼2.0. UV−vis measurements were performed at room temperature using 1-cm optical path length cuvettes and an Agilent Technologies 8453 GA11034 spectrophotometer. Aliquots removed from experiments performed at 90 °C were cooled by holding the cuvette under running tap water for 3 min prior to the measurements. In the UV irradiation study, a long wave ultraviolet lamp (unfiltered) placed in a dark box was used to irradiate sample mixtures. The spectrum of the UV lamp used is provided in Figure SI-1 (Supporting Information (SI)). The intensity of the UV light was 21 700 $\mu W/cm^2$ at a distance of 5 cm according to specifications provided by the manufacturer. The solutions of Ag^+−FA and Ag^+−HA were placed at a distance of about 15 cm from the light source and were irradiated for 1 h at a lamp intensity of 2411 $\mu W/cm^2$. The UV measurements of samples were taken at 15-min time intervals.

Characterization of AgNPs. The size distributions of Ag NPs were investigated by dynamic light scattering (DLS) using a Zetasizer Nano Series (Malvern Instruments) instrument. The same instrument was also used to measure zeta potentials in aqueous dispersions using patented M3-PALS (phase analysis light scattering) technology. Morphologies of AgNPs were determined by employing JEOL JEM-2010 transmission electron microscopy (TEM) equipped with a LaB_6 cathode (accelerating voltage of 160 kV; a point-to-point resolution of 0.194 nm). Briefly, a drop of the sample solution was placed onto a holey-carbon film supported by a copper grid and allowed to dry in air at room temperature before performing TEM measurements. FT-IR absorption spectra were measured at room temperature under ambient conditions on an iS5 spectrometer (Nicolet Thermo Scientific) using attenuated total reflection (ATR) (ZnSe crystal, 64 scans and 2 cm^{-1} resolution). Spectra were recalculated from reflectance to absorbance, were baseline corrected, and are presented in transmittance mode. X-ray photoelectron spectroscopy (XPS) was performed on a Phi 5000 VersaProbe instrument using monochromatic Al Kα X-rays with charge neutralization. The solutions were drop cast onto cleaned silicon chips, dried in air overnight, and then used for the XPS measurements. The silver $3d_{5/2}$ and $3d_{3/2}$ binding energies were calibrated with the spectrum acquired for a $AgNO_3$ standard, which was referenced to the National Institute of Standards and Technology (NIST) XPS database.[25]

RESULTS AND DISCUSSION

Formation and Characterization of AgNPs. In initial experiments, AgNPs were formed by mixing Ag^+ with SRFA at pH 8.0 at room temperature (RT). The characteristic intense yellow color due to the surface plasmon resonance (SPR) of AgNPs gradually appeared over a period of days. The spectra collected over different days are presented in Figure SI-2 (SI). Similar experiments were performed by heating the reaction mixture at 90 °C for 2 h; the spectra obtained at different time intervals are shown in Figure SI-2. Control spectra in which no Ag^+ ions were present are also shown in Figures 1 and SI-2. Absorbance peaks of AgNPs were not influenced by the absorbance of SRFA. The characteristic peaks of AgNPs were

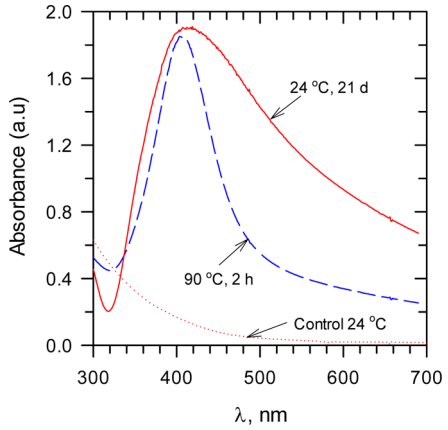

Figure 1. UV−vis absorption spectra of AgNPs in SRFA at different temperatures and pH 8.0. ($[Ag^+]$ = 1 × 10^{-3} mol L^{-1}, 100 mg L^{-1} SRFA).

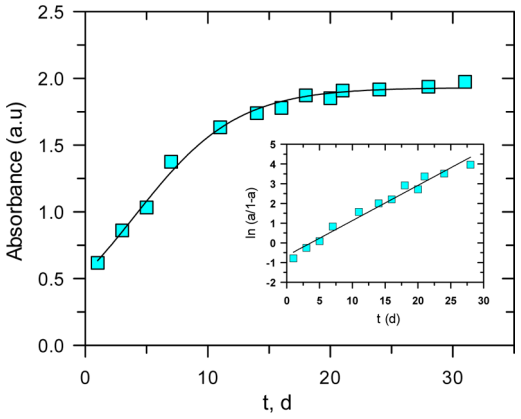

Figure 2. Plot of absorbance versus time for the formation of AgNPs at 22 °C ($[Ag^+]$ = 1 × 10^{-3} mol L^{-1}, 100 mg L^{-1} SRFA). Inset: Plot of $\ln(\alpha/1-\alpha)$ versus time.

similar to those observed in the humic acid-mediated reduction of Ag^+ to AgNPs.[17] The TEM and its diffraction (*d*-spacings) spectra of AgNPs confirmed the presence of crystalline AgNPs that were not present in the control. The similarity of functional groups (Table SI-1) and likely reduction processes of FAs and HAs support the conclusion that the SPR peaks in the present study are indeed those of AgNPs. A comparison of AgNP growth characteristics is shown by contrasting spectra acquired for AgNP samples formed at the two temperatures (Figure 1). The SPR peaks of AgNPs were both centered at approximately 400 nm; however, the SPR peaks of AgNPs formed at room temperature had a broader absorption feature, whereas a sharper absorption was observed for the AgNPs formed at 90 °C (Figure 1). At high temperatures, initially formed molecular Ag-precursors (presumably bound to FA) likely form larger clusters, which undergo dissolution, recrystallization, and surface reconstruction to yield AgNPs with well-defined surface plasmon resonances. These absorption features are readily discernible in optical absorption spectra upon cooling after 2 h of heating. In contrast, AgNPs are formed only after a period of several days at RT and much broader peaks are evidenced, suggesting considerable polydispersity in size and local dielectric environment.

A plot of the increase in the absorbance as a function of time suggests an autocatalytic process (Figure 2) for Ag NP growth. The following equation thus may be written for this process.

$$Ag^+ + Ag_n + FA \rightarrow Ag_{n+1} + FA(ox) \quad (1)$$

Ag^+ ions from the bulk solution adsorb onto a small cluster Ag_n, which further catalyzes the growth of AgNPs. In this process, Ag^+ ions are reduced by SRFA. The following equation for the autocatalytic process can be written as[26]

$$\ln(a/(1-a)) = (k[Ag^+])t - \ln([Ag^+]/n[Ag_n]) \quad (2)$$

where $a = A_t/A_\infty$, and A_t and A_∞ are the absorbance values at time t and ∞, respectively. Variation of ln $(a/(1-a))$ with the reaction time yields a linear relationship (Figure 2, inset). This supports the idea that the formation of AgNPs in the Ag^+−FA mixture results from an autocatalytic reaction.

Next, the effect of varying concentrations of Ag^+ and SRFA on the formation of AgNPs was studied at 90 °C. The SPR features increase with increasing concentrations of Ag^+ ions and SRFA in the reaction mixtures (Figure 3a and b). Optical absorption spectra for SRFA without any addition of Ag^+ at natural pH are shown in Figure SI-3. The rate of the formation of AgNPs clearly depends on both the concentrations of Ag^+ ions and SRFA. The broadening of peaks with lower concentration of either Ag^+ ions or SRFA was also observed. This may be due to insufficient amounts of either of the reactive species for stabilization of small diameter AgNPs. In the absence of an adequate flux of Ag^+ ions or the reducing agent, the growth rates are likely limited by precursor diffusion. In the absence of Ostwald ripening and focusing of size, a fairly polydisperse range of AgNPs is obtained. An increase in growth rate of AgNPs was also observed with increase in pH at 90 °C (Figure 3c); SPR peaks of AgNPs also broadened with decreasing pH (Figure 3c).

The formation of AgNPs through the direct reduction of Ag^+ ions by SRFA is not thermodynamically feasible. The redox potential for FA is ∼0.5 V, which is not sufficient to overcome the highly negative redox potential of Ag^+ ions to isolated silver ($Ag^+ + e^- \rightarrow Ag^o$; E^o = −1.8 V vs NHE).[27] However, it is possible that Ag^+ ions deposited onto stable clusters or solid surfaces are being reduced by SRFA due to a more positive redox potential. For example, the redox potential for reducing Ag^+ onto a Ag electrode is +0.8 V.[28] In our study, adsorption of Ag^+ ions may be occurring onto colloidal Ag_2O, which is likely generated as a transient species through reaction 3. It should be

$$2\,Ag^+ + 2OH^- \rightarrow Ag_2O + H_2O \quad \text{fast} \quad (3)$$

$$Ag_2O + (Ag^+)_n \rightarrow Ag_2O\text{-}(Ag^+)_n \quad \text{fast} \quad (4)$$

$$Ag_2O\text{-}(Ag^+)_n + FA \rightleftharpoons Ag_2O\text{-}(Ag^+)_n\text{-}FA \quad K_{ad} \quad (5)$$

$$Ag_2O\text{-}(Ag^+)_n\text{-}FA \rightarrow Ag_2O\text{-}(Ag^+)_{n-1} + Ag^o + FA^-(ox) \quad k_{red} \quad (6)$$

$$Ag^o + Ag^o \rightarrow Ag_2 \quad \text{fast} \quad (7)$$

pointed out that reaction 3 would not result in the formation of AgOH because Ag^+ ion does not hydrolyze under the mild alkaline conditions of the present study.[26] Reaction 3 could be immediately followed by the fast generation of colloidal Ag_2O−$(Ag^+)_n$ particles (reaction 4). It is proposed that SRFA adsorbs onto these colloidal particles (reaction 5), prior to the reduction step in which metallic silver is formed and FA is oxidized (reaction 6). The dimerization of metallic silver is proposed in reaction 7. A recent study suggests that silver dimer formation can occur on the time scale of milliseconds.[29] While the formation of dimers has specifically been illustrated,

dx.doi.org/10.1021/es302305f | *Environ. Sci. Technol.* 2013, 47, 757−764

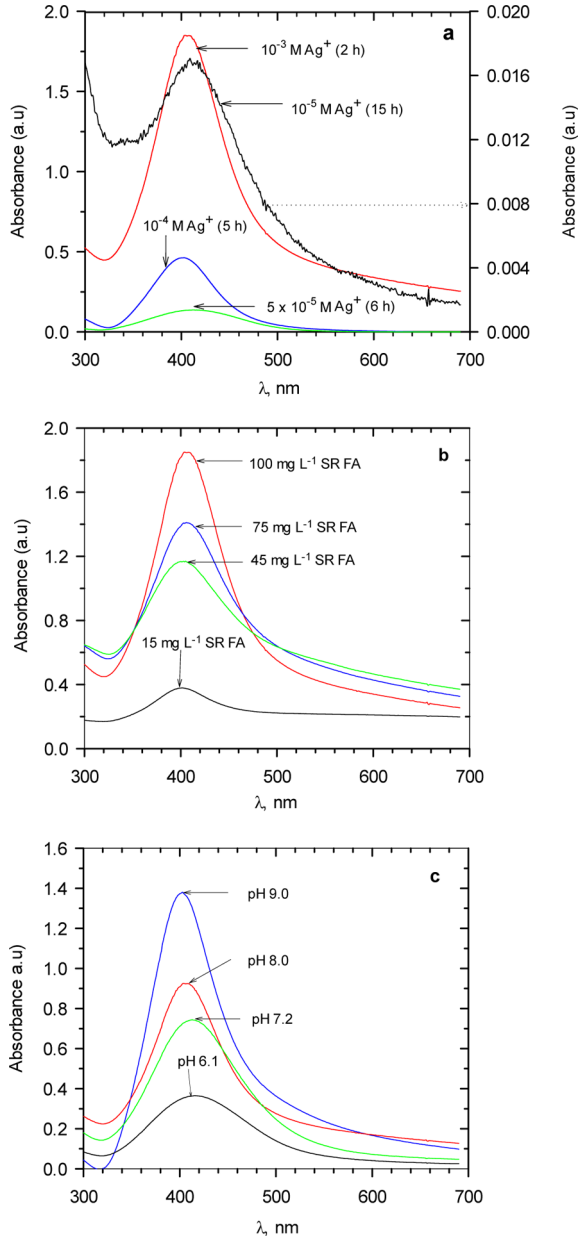

Figure 3. UV−vis absorption spectra of AgNPs in SRFA at 2 h heating at 90 °C. (a) Different concentrations of Ag^+ (100 mg L^{-1} SRFA; pH 8.0); (b) different concentrations of SRFA ($[Ag^+] = 1 \times 10^{-3}$ mol L^{-1}, pH 8.0); and (c) different pH ($[Ag^+] = 1 \times 10^{-3}$ mol L^{-1}, 100 mg L^{-1} SRFA).

similar principles are applicable to the stabilization of larger clusters. For instance, the formation of metastable Ag_{13} clusters has been found to proceed on a millisecond time scale upon the reduction of Ag^+ by citrate.[30] The autocatalytic reduction of Ag^+ may represent the driving force to reach metastable (or "magic-sized") Ag_n clusters that are thermodynamically far more favored than smaller entities. These metastable silver clusters agglomerate during the growth period and produce the characteristic yellow color of AgNPs.

In the proposed mechanism, reaction step 6 is the rate-determining step and the reduction capacity of FA therefore determines the amount of metallic silver formed. The posited mechanistic steps (reactions 3−7) suggest that the growth of AgNPs should be directly related to the concentrations of both Ag^+ ions and SRFA as is indeed borne out experimentally (Figure 3a and b). An increase in the pH of the reaction may be causing two favorable processes that potentially enhance AgNP growth (Figure 3c). The higher concentration of OH^- ions in solution would increase the formation of colloidal Ag_2O and hence increase the rate of formation of $Ag_2O-(Ag^+)_n$ particles. Also at higher pH, the functional groups of aromatic fractions of FA should occur mainly as deprotonated species, with relatively higher electron density compared to functional groups of protonated species. This is expected to facilitate initial binding and complexation of Ag^+ ions by FA species. Such coordination likely precedes nucleation of Ag clusters and thus increased pH is equivalent to an increased concentration of nucleation sites. Both of these processes likely contribute to increasing the rate of the formation of AgNPs at higher pH (Figure 3c). In the slightly acidic environment (i.e., pH 6.1), the formation of AgNPs would thus not be favorable, which has also been borne out by our experimental results.

The formation of Ag_2O in the proposed mechanism was explored by performing XPS measurements on the dehydrated powder obtained from the mixed solutions of Ag^+ and SRFA at 90 °C. The XPS spectra are shown in Figure SI-4. The Ag $3d_{5/2}$ and $3d_{3/2}$ components appeared at 367.2 and 373.1 eV, respectively, which indicate an oxidized form of Ag (and not metallic Ag).[31,32] However, variations in binding energies of different oxidation states of Ag is very minor (ca. 0.2 eV), which made it difficult to positively conclude the presence of Ag_2O. But it is clear from the XPS data that the nanoparticle surfaces were oxidized; suggesting either the presence of Ag_2O or FA-coordinated ionic Ag species.

The formation of AgNPs was studied using different FAs and HA at pH 8.0 and 90 °C. Control spectra of FAs and HA are plotted in Figure SI-5. SRHA yields AgNPs at an accelerated rate as compared to SRFA (Figure 4). The relative ordering of

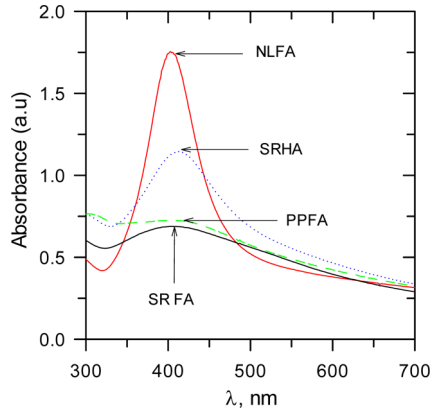

Figure 4. UV−vis absorption spectra of AgNPs for different FAs and SRHA at pH 8.0. (SRFA, Suwannee River fulvic acid I; SRPP, Suwannee River Pahokee Peat II; SRNL, Suwannee River Nordic Lake; SRHA, Suwannee River II humic acid) ($[Ag^+] = 1 \times 10^{-3}$ mol L^{-1}, 45 mg L^{-1} fulvic and humic acids, heating at 90 °C for 2 h).

AgNP growth rate has been determined to be NLFA > SRHA > PPFA > SRFA. As expected, peak broadening follows the reverse trend (Figure 4). The relative predilection of the different natural organic matter components for facilitating AgNP growth can be understood by considering the individual components present in FAs and in SRHA as summarized by the IHSS (Table SI-1). The functional groups and carbon distributions present in the samples do not show a clear

dx.doi.org/10.1021/es302305f | Environ. Sci. Technol. 2013, 47, 757−764

correlation with ordering of AgNP growth rates. However, the free radical content of the samples can be correlated with the rate of formation of AgNPs. Free radical content of the samples followed the order NLFA > SRHA > SRFA, which indeed is correlated to the experimentally determined growth rates for formation of AgNPs. It thus appears that free radical species may be involved in the rate-controlling reduction step that results in the initial formation of metallic silver (reaction 6). Fulvic and humic acids have moieties such as semiquinones,[33] possibly providing free radical character capable of reducing Ag^+ onto colloidal Ag_2O particles. Additionally, other chemical species such as thiols, phenolic, and carboxylic groups in the FAs and HA may also influence the formation of AgNPs.

Influence of UV Light. In this set of experiments, mixtures of Ag^+−FAs and Ag^+−HA in MHRW at pH 8.0 were illuminated with UV light for 1 h. Without the UV-irradiation, AgNPs did not form in 1 h (Figure 5). Exposure to UV light

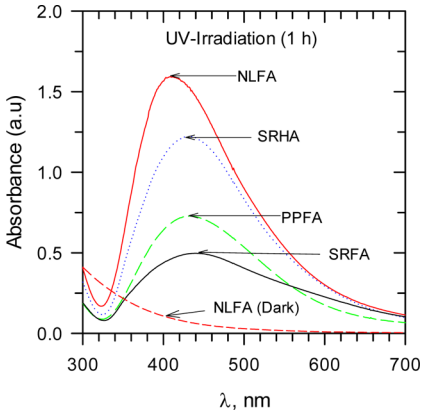

Figure 5. UV−vis absorption spectra of AgNPs formed in MHRW synthetic freshwater under UV irradiation for 1 h at pH 8.0. (([Ag^+] = 1×10^{-3} mol L^{-1}, FA or HA = 45 mg L^{-1}).

resulted in the formation of the characteristic yellow color of AgNPs. The photochemical growth of AgNPs has been previously reported in the presence of photosensitizers in solution.[29,34] It appears that both fulvic and humic acids in the reaction mixtures of the present study act as photosensitizers for the formation of AgNPs. Ag_2O may behave like a semiconductor.[35] The photoreduction of Ag^+ adsorbed onto Ag_2O by the reactive species produced in solution may also be responsible for the formation of AgNPs. These species include hydrated electrons and $O_2^{-\bullet}$,[36,37] which have been independently shown to reduce Ag^+ ions to yield AgNPs.[38] Another photochemically produced species, H_2O_2[39] may oxidize AgNPs back to Ag^+.[38] Overall, the interactions among Ag^+, AgNPs, and reactive species are determining the formation of AgNPs.[38] A comparison of AgNP growth under UV light in the presence of different fulvic and humic acids is presented in Figure 5. Control spectra are presented in Figure SI-6. The rate of photochemically induced growth of AgNPs followed the order NLFA > SRHA > PPFA > SRFA; similar to the trend observed upon heating the samples at 90 °C. This suggests that the reducing capacity of the acids also has an effect on the photochemical growth of AgNPs.

Stability of AgNPs. Experiments were performed on the stability of SRFA-formed AgNPs for several months under normal laboratory conditions (Figure 6). The AgNPs were stored in capped vials throughout the period of the study, however vials were periodically opened to remove aliquots for UV−vis spectral measurements of the sample. In Figure 6a, the set of UV−vis spectra of samples formed by the mixing of Ag^+ and SRFA at room temperature are shown, in which days are counted from the solution preparation (AgNPs-RT). In Figure 6b, days represent the period of time after formation of AgNPs by heating at 90 °C for 2 h (AgNPs-90). Obviously, there were distinct differences in the UV−vis absorption characteristics of AgNPs-RT (Figure 6a) and AgNPs-90 (Figure 6b) over a period of time. AgNPs obtained under RT conditions showed no significant changes 48 days after their formation. However, after 180 days, a decrease in absorbance of the SPR peak (∼15%) is discernible. Significantly, the SPR feature does not show any broadening during this period of time (Figure 6a). In contrast, AgNPs formed at 90 °C indicated continuous broadening of the SPR peak with time (Figure 6b), perhaps suggestive of agglomeration and increased polydispersity, which likely indicates a difference in stability, which is correlated to the surface passivation of the particles and their mode of binding FA. The SPR peak absorbance value for AgNPs-90 after 210 days had a similar percentage decrease as was observed for AgNPs-RT after 180 days.

It is clear that the process of AgNP nucleation was rather slow at RT while more pronounced nucleation occurred at the elevated temperature (90 °C). Furthermore, when AgNP aggregation and/or growth occurred, there were clearly changes in particle size distributions, which resulted in broadening of the SPR peak. Significantly, the final SPR bands were similar in intensity and broadness for AgNPs-RT after 180 days (Figure 6a) compared to AgNPs-90 after 210 days (Figure 6b). Dynamic light scattering (DLS) measurements were carried out for AgNPs-RT (Figure 6c and 6e) and AgNPs-90 (Figure 6d and 6f) after 180 and/or 210 days, respectively, in order to confirm size distributions of particles dispersed in these samples. Figure 6c−6f show size distributions based on intensity and number. Bimodal distributions based on intensity fluctuation measurements in both samples were observed (Figure 6c and 6d), which suggest the presence of two size fractions: large (∼146 nm average size for AgNPs-RT and ∼133 nm average size for AgNPs-90) and small (∼12 nm average size for AgNPs-RT and ∼8 nm average size for AgNPs-90) particles. TEM images of AgNPs-RT and AgNPs-90 aged for several months (Figure 6g and 6h) also corroborate DLS results, i.e. a rather broad particle size distribution with two distinct maxima of average nanoparticle sizes above 100 nm and below 10 nm in diameter.

The FA residues on the AgNPs shown in Figure 6c−6h were further characterized by FT-IR absorption spectroscopy (Figure SI-7). There was no distinct difference in the two AgNPs FT-IR spectra (Figure SI-7): stretching vibrations for CH (2957, 2922, 2852 cm^{-1}) and CO (1740, 1610, 1410, 1165 cm^{-1}) could be recognized in addition to the bands stemming from the buffer solution (borate, hydrogenphosphate, dihydrogenphosphate), which were assigned on the basis of literature values.[40,41] The positions and relative intensities of IR absorption peaks are the same in both samples, which indicates that the reduction of Ag^+ ions induces possible oxidative changes in SRFA (whose IR spectrum in the same buffer solution is directly compared in Figure SI-6 as well) to the same extent regardless of the temperature. Comparing the FT-IR absorption spectrum of SRFA with and without the presence of AgNPs (Figure SI-7), a significant increase of the CH stretching vibration signal (the region between 3000 and 2800 cm^{-1}) together with an

dx.doi.org/10.1021/es302305f | Environ. Sci. Technol. 2013, 47, 757−764

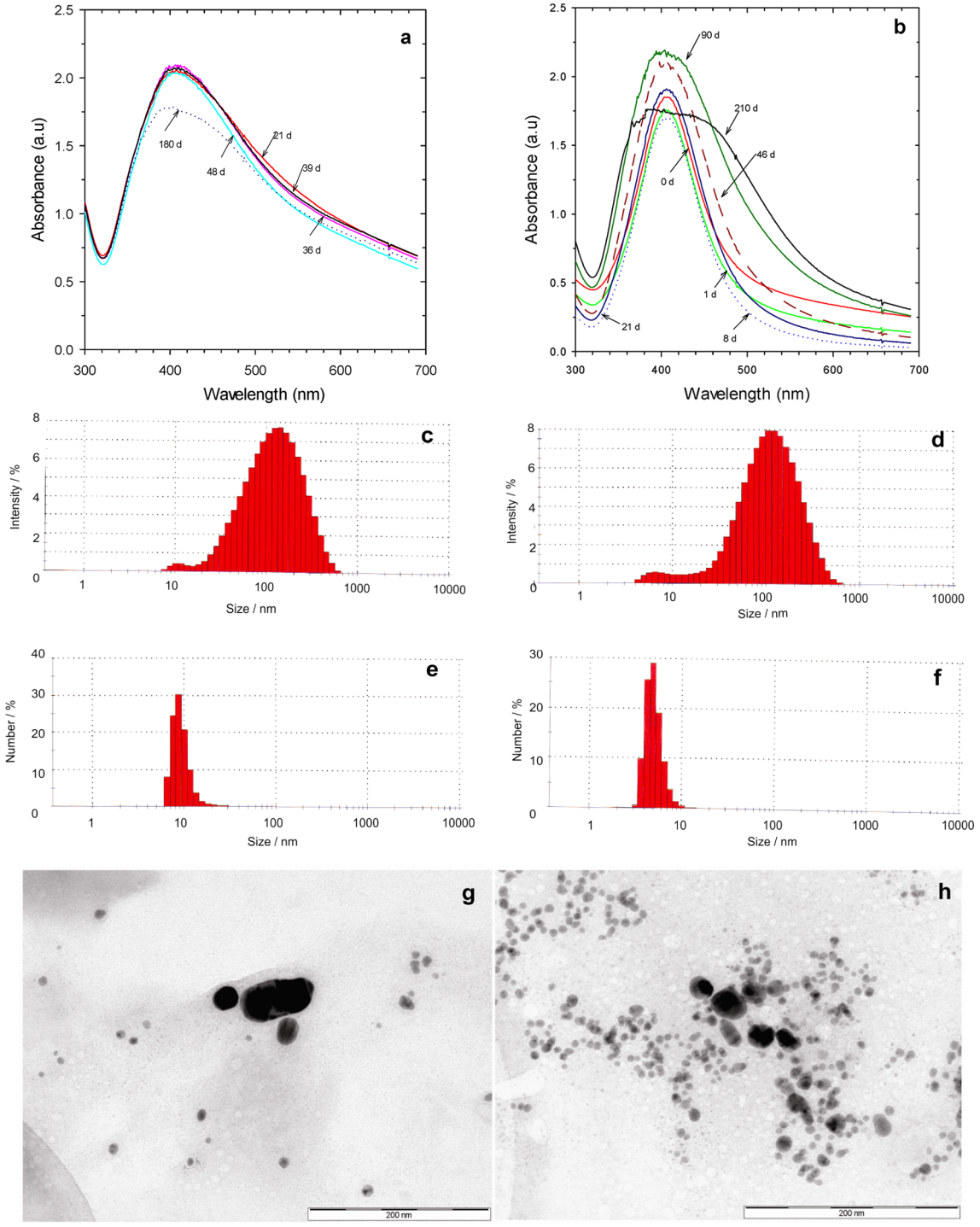

Figure 6. Aging of AgNPs prepared at RT (a, c, e, g) and 90 °C (b, d, f, h): UV−vis, DLS measurements, and TEM images of AgNPs following reduction of Ag^+ ion by SRFA. (Conditions: $[Ag^+] = 1 \times 10^{-3}$ mol L^{-1}, 100 mg L^{-1} SRFA; pH 8.0. (Days in (a) present after initial mixing of Ag^+−SRFA while days in (b) represents after forming of AgNPs at 90 °C for 2 h). (a) UV−vis spectra of the samples prepared at RT followed in time; (b) UV−vis spectra of the samples prepared at 90 °C followed in time; DLS determined size distributions based on intensity fluctuation (c, d) and on particle number (e, f) of AgNPs-RT after 180 days and/or AgNPs-90 after 210 days; (g, h) TEM images of the same samples as in c−f.

increased intensity of the bands attributed to aromatic C═C (1600−1450 cm^{-1}) and COO^- (positioned at ∼1410 and ∼1610 cm^{-1}) can be seen. The increased intensity of all of the above-mentioned bands can be induced by the formation of AgNPs and the adsorption of SRFA onto their surfaces. Due to the presence of the surface plasmon resonance of AgNPs, all optical processes are enhanced, i.e. including absorption.[42] Moreover, the increased intensity of the ∼1410 cm^{-1} band (symmetric COO^- stretch) in comparison to that of the ∼1610 cm^{-1} band (asymmetric COO^- stretch and aromatic C═C) may be explained by a complexation of carboxylic groups of SRFA with silver on the AgNP surface similar to that which has been observed for humic acid adsorption on goethite.[43,44]

It seems that the adsorption of SRFA onto AgNPs is possibly inhibiting the coagulation of the AgNP suspension. The zeta potential of AgNPs after 3 days was −40 mV. Also, the zeta

dx.doi.org/10.1021/es302305f | Environ. Sci. Technol. 2013, 47, 757−764

potentials of AgNPs-RT after 180 days and AgNPs-90 after 210 days were measured as −27 mV and −33 mV, respectively, supporting the likelihood of repulsive forces between negatively charged particles, preventing the aggregation of AgNPs.

Environmental Implications. The results suggest that formation of AgNPs in the aquatic environment is highly dependent on pH and temperature, controlling the size and shape of AgNPs. Environmentally relevant concentrations of FA (15 mg L^{-1}) and pH (7.4−8.1, RT) can potentially form AgNPs in natural waters. Significantly, higher concentrations of dissolved silver and elevated temperatures, conditions usually seen in hot-springs and thermal vents, would also increase the potential for formation of AgNPs. Interactions of Ag^+ with organic matter would also be influenced by the ionic strength.[45] The UV-irradiated studies indicate the possible formation of AgNPs in surface waters where natural organic matter and solar light are present, if sufficient concentrations of Ag^+ are available. Preliminary studies in which a mixture of Ag^+−SRFA was kept under solar light for 8 h resulted in the formation of AgNPs (Figure SI-8). The photochemistry of organic matter and the subsequent generation of reactive species would thus play an important role in the formation of AgNPs in the natural environment. This complex phenomenon of AgNP generation needs further investigation.

The stability of AgNPs influences their mobility, bioavailability, and toxicity in the environment.[7,46] The AgNPs in the present study are very stable for many months in contrast to citrate-coated engineered AgNPs, which aggregate within hours. However, $NaBH_4$-synthesized AgNPs have been reported to be stable for a few months.[16] The adsorption of BH_4^- anions onto AgNPs creates a negative zeta potential (−39 mV), similar to values found in our study. The presence of high molecular weight organic matter on the surface of nanoparticles is likely preventing the aggregation and as such AgNPs could be transported significant distances from their point of origin. Furthermore, the demonstrated stability of AgNPs in Ag^+−FA aqueous solutions suggests that surfaces of nanoparticles are sufficiently covered to an extent that inhibits the dissolution of the nanoparticles by oxygen to release silver ion. The toxicity due to the release of Ag^+ from organic matter coated-AgNPs should be less than that of engineered AgNPs. However, surface charge on nanoparticles also needs to be considered to better understand their toxic behavior.[14] Some studies on the toxic effect of engineered AgNPs in the presence of humic and fulvic acids have been carried out, but knowledge of the adverse effects of natural organic matter-coated AgNPs on organisms is lacking. The effect of solar light on the stability and dissolution of engineered AgNPs and naturally formed AgNPs at the present time is almost unknown. This variable needs to be considered when characterizing AgNP transformations under realistic environmental conditions. Future work will focus on elaboration of mechanistic aspects of the photochemical reduction of Ag^+.

■ ASSOCIATED CONTENT

Supporting Information

Additional information as noted in the text. This material is available free of charge via the Internet at http://pubs.acs.org.

■ AUTHOR INFORMATION

Corresponding Author

*Phone: 321-674-7310; fax: 321-674-8951; e-mail: vsharma@fit.edu.

Notes

The authors declare no competing financial interest.

■ ACKNOWLEDGMENTS

V.K.S. and M.S. wish to thank the Chemistry Endowment at Florida Tech. K.S. and R.Z. acknowledge the support by project P108/11/P657 awarded by Grant Agency of the Czech Republic, the Operational Program Education for Competitiveness—European Social Fund (CZ.1.07/2.3.00/20.0056), Operational Program Research and Development for Innovations − European Regional Development Fund (project CZ.1.05/2.1.00/03.0058 of the Ministry of Education, Youth and Sports of the Czech Republic). We also thank Dr. Klara Safarova for assistance with TEM images at the Regional Centre of Advanced Technologies and Materials at Olomouc, Czech Republic. We sincerely thank the anonymous reviewers for their comments, which significantly improved the paper.

■ REFERENCES

(1) Woodrow Wilson International Center for Scholars. *Consumer Products: An Inventory of Nanotechnology-based Consumer Products currently on the Market, 2010*; 2010; www.nanotechproject.org/inventories/consumer/.

(2) Nadagouda, M. N.; Speth, T. F.; Varma, R. S. Microwave-assisted green synthesis of silver nanostructures. *Acc. Chem. Res.* **2011**, *44*, 469−478.

(3) Nowack, B.; Krug, H. F.; Height, M. 120 years of nanosilver history: Implications for policy makers. *Environ. Sci. Technol.* **2011**, *45*, 1177−1183.

(4) Dallas, P.; Sharma, V. K.; Zboril, R. Silver polymeric nanocomposites as advanced antimicrobial agents: Classification, synthetic paths, applications, and perspectives. *Adv. Colloid Interface Sci.* **2011**, *166*, 119−135.

(5) Sharma, V. K.; Yngard, R. A.; Lin, Y. Silver nanoparticles: Green synthesis and their antimicrobial activities. *Adv. Colloid Interface Sci.* **2009**, *145*, 83−96.

(6) Rico, C. M.; Majumdar, S.; Duarte-Gardea, M.; Peralta-Videa, J. R.; Gardea-Torresdey, J. L. Interaction of nanoparticles with edible plants and their possible implications in the food chain. *J. Agric. Food Chem.* **2011**, *59*, 3485−3498.

(7) Levard, C.; Hotze, E. M.; Lowry, G. V.; Brown, G. E. Environmental transformations of silver nanoparticles: Impact on stability and toxicity. *Environ. Sci. Technol.* **2012**, *46*, 6900−6914.

(8) Peralta-Videa, J. R.; Zhao, L.; Lopez-Moreno, M. L.; de la Rosa, G.; Hong, J.; Gardea-Torresdey, J. L. Nanomaterials and the environment: A review for the biennium 2008−2010. *J. Hazard. Mater.* **2011**, *186*, 1−15.

(9) Mukherjee, B.; Weaver, J. W. Aggregation and charge behavior of metallic and nonmetallic nanoparticles in the presence of competing similarly-charged inorganic ions. *Environ. Sci. Technol.* **2010**, *44*, 3332−3338.

(10) Chinnapongse, S. L.; MacCuspie, R. I.; Hackley, V. A. Persistence of singly dispersed silver nanoparticles in natural freshwaters, synthetic seawater, and simulated estuarine waters. *Sci. Total Environ.* **2011**, *409*, 2443−2450.

(11) Thio, B. J. R.; Montes, M. O.; Mahmoud, M. A.; Lee, D.; Zhou, D.; Keller, A. A. Mobility of Capped Silver Nanoparticles under Environmentally Relevant Conditions. *Environ. Sci. Technol.* **2012**, *46*, 6985−6991.

(12) Gebauer, J. S.; Treuel, L. Influence of individual ionic components on the agglomeration kinetics of silver nanoparticles. *J. Colloid Interface Sci.* **2011**, *354*, 546−554.

(13) Piccapietra, F.; Sigg, L.; Behra, R. Colloidal stability of carbonate-coated silver nanoparticles in synthetic and natural freshwater. *Environ. Sci. Technol.* **2012**, *46*, 818−825.

(14) El Badawy, A. M.; Luxton, T. P.; Silva, R. G.; Scheckel, K. G.; Suidan, M. T.; Tolaymat, T. M. Impact of environmental conditions

(pH, ionic strength, and electrolyte type) on the surface charge and aggregation of silver nanoparticles suspensions. *Environ. Sci. Technol.* **2010**, *44*, 1260−1266.
(15) Aiken, G. R.; Hsu-Kim, H.; Ryan, J. N. Influence of dissolved organic matter on the environmental fate of metals, nanoparticles, and colloids. *Environ. Sci. Technol.* **2011**, *45*, 3196−3201.
(16) Delay, M.; Dolt, T.; Woellhaf, A.; Sembritzki, R.; Frimmel, F. H. Interactions and stability of silver nanoparticles in the aqueous phase: Influence of natural organic matter (NOM) and ionic strength. *J. Chromatogr. A* **2011**, *1218*, 4206−4212.
(17) Akaighe, N.; MacCuspie, R. I.; Navarro, D. A.; Aga, D. S.; Banerjee, S.; Sohn, M.; Sharma, V. K. Humic acid-induced silver nanoparticle formation under environmentally relevant conditions. *Environ. Sci. Technol.* **2011**, *45*, 3895−3901.
(18) Figueroa, J. A. L.; Wrobel, K.; Afton, S.; Caruso, J. A.; Felix Gutierrez Corona, J.; Wrobel, K. Effect of some heavy metals and soil humic substances on the phytochelatin production in wild plants from silver mine areas of Guanajuato, Mexico. *Chemosphere* **2008**, *70*, 2084−2091.
(19) Eckelman, M. J.; Graedel, T. E. Silver emissions and their environmental impacts: A multilevel assessment. *Environ. Sci. Technol.* **2007**, *41*, 6283−6289.
(20) Kramer, D.; Cullen, J. T.; Christian, J. R.; Johnson, W. K.; Pedersen, T. F. Silver in the subarctic northeast Pacific Ocean: Explaining the basin scale distribution of silver. *Mar. Chem.* **2011**, *123*, 133−142.
(21) Wen, L.-.; Santschi, P. H.; Gill, G. A.; Paternostro, C. L.; Lehman, R. D. Colloidal and particulate silver in river and estuarine waters of Texas. *Environ. Sci. Technol.* **1997**, *31*, 723−731.
(22) Gómez-Caballero, J. A.; Villaseñor-Cabral, M. G.; Santiago-Jacinto, P.; Ponce-Abad, F. Hypogene Ba-rich todorokite and associated nanometric native silver in the San Miguel Tenango mining area, Zacatlán, Puebla, Mexico. *Can. Mineral.* **2010**, *48*, 1237−1253.
(23) Sal'nikov, D. S.; Pogorelova, A. S.; Makarov, S. V.; Vashurina, I. Y. Silver ion reduction with peat fulvic acids. *Russ. J. Appl. Chem.* **2009**, *82*, 545−548.
(24) U.S. Environmental Protecion Agency. *Methods for Measuring the Acute Toxicity of Effluents and Receiving Waters to Freshwater and Marine Organisms, Highlights of 600/4-90/027F*; 1993; www.epa.gov/waterscience/methods/wet/disk2/atx.pdf.
(25) NIST X-ray Photoelectron Spectroscopy Database, Version 3.5 2003.
(26) Huang, Z.-.; Mills, G.; Hajek, B. Spontaneous formation of silver particles in basic 2-propanol. *J. Phys. Chem.* **1993**, *97*, 11542−11550.
(27) Gentry, S. T.; Fredericks, S. J.; Krchnavek, R. Controlled particle growth of silver sols through the use of hydroquinone as a selective reducing agent. *Langmuir* **2009**, *25*, 2613−2621.
(28) Henglein, A. Non-metallic silver clusters in aqueous solution: stabilization and chemical reactions. *Chem. Phys. Lett.* **1989**, *154*, 473−476.
(29) Stamplecoskie, K. G.; Scaiano, J. C. Silver as an Example of the Applications of Photochemistry to the Synthesis and Uses of Nanomaterials. *Photochem. Photobiol.* **2012**, *88*, 762−768.
(30) Takesue, M.; Tomura, T.; Yamada, M.; Hata, K.; Kuwamoto, S.; Yonezawa, T. Size of elementary clusters and process period in silver nanoparticle formation. *J. Am. Chem. Soc.* **2011**, *133*, 14164−14167.
(31) Dong, T.-Y.; Chen, W.-T.; Wang, C.-W.; Chen, C.-P.; Chen, C.-N.; Lin, M.-C.; Song, J.-M.; Chen, I.-G.; Kao, T.-H. One-step synthesis of uniform silver nanoparticles capped by saturated decanoate: Direct spray printing ink to form metallic silver films. *Phys. Chem. Chem. Phys.* **2009**, *11*, 6269−6275.
(32) Tan, Y.; Wang, Y.; Jiang, L.; Zhu, D. Thiosalicylic acid-functionalized silver nanoparticles synthesized in one-phase system. *J. Colloid Interface Sci.* **2002**, *249*, 336−345.
(33) Aeschbacher, M.; Graf, C.; Schwarzenbach, R. P.; Sander, M. Antioxidant properties of humic substances. *Environ. Sci. Technol.* **2012**, *46*, 4916−4925.
(34) Sudeep, P. K.; Kamat, P. V. Photosensitized growth of silver nanoparticles under visible light irradiation: A mechanistic investigation. *Chem. Mater.* **2005**, *17*, 5404−5410.
(35) Tselepis, E.; Fortin, E. Preparation and photovoltaic properties of anodically grown Ag_2O films. *J. Mater. Sci.* **1986**, *21*, 985−988.
(36) Wang, W.; Zafiriou, O. C.; Chan, I.-.; Zepp, R. G.; Blough, N. V. Production of hydrated electrons from photoionization of dissolved organic matter in natural waters. *Environ. Sci. Technol.* **2007**, *41*, 1601−1607.
(37) Jones, A. M.; Garg, S.; He, D.; Pham, A. N.; Waite, T. D. Superoxide-mediated formation and charging of silver nanoparticles. *Environ. Sci. Technol.* **2011**, *45*, 1428−1434.
(38) He, D.; Jones, A. M.; Garg, S.; Pham, A. N.; Waite, T. D. Silver nanoparticle-reactive oxygen species interactions: Application of a charging-discharging model. *J. Phys. Chem. C* **2011**, *115*, 5461−5468.
(39) Burns, J. M.; Cooper, W. J.; Ferry, J. L.; King, D. W.; DiMento, B. P.; McNeil, K.; Miller, C. J.; Miller, W. L.; Peake, B. M.; Rusak, S. A.; Rose, A. L.; Waite, T. D. Methods for reactive oxygen species (ROS) detection in aqueous environments. *Aquatic Sci.* **2012**, *74*, 683−734.
(40) Nakamoto, K. *Infrared and Raman Spectra of Inorganic and Coordination Compounds, Part A*; John Wiley & Sons Inc.: Hoboken, NJ, USA,ISBN 978-0-471-74339-2, 2009; pp 285−287 and 388−392.
(41) Nakamoto, K. *Infrared and Raman Spectra of Inorganic and Coordination Compounds, Part B*; John Wiley & Sons Inc.: Hoboken, NJ, USA, ISBN 978-0-471-74339-1, 2009; pp 62−67.
(42) LeRu, E. C.; Etchegoin, P. G. *Principles of Surface-Enhanced Raman Spectroscopy and Related Plasmonic Effects*; Elsevier: Linacre House, Jordan Hill, Oxford, UK, 2009.
(43) Ghosh, S.; Jiang, W.; McClements, J. D.; Xing, B. Colloidal stability of magnetic iron oxide nanoparticles: Influence of natural organic matter and synthetic polyelectrolytes. *Langmuir* **2011**, *27*, 8036−8043.
(44) Kang, S.; Xing, B. Humic acid fractionation upon sequential adsorption onto goethite. *Langmuir* **2008**, *24*, 2525−2531.
(45) Akaighe, N.; Depner, S. W.; Banerjee, S.; Sharma, V. K.; Sohn, M. The effects of monovalent and divalent cations on the stability of silver nanoparticles formed from direct reduction of silver ions by Suwannee river humic acid/natural organic matter. *Sci. Total Environ.* **2012**, *441*, 277−289.
(46) Xiu, Z. M.; Ma, J.; Alvarez, P. J. J. Differential effect of common ligands and molecular oxygen on antimicrobial activity of silver nanoparticles versus silver ions. *Environ. Sci. Technol.* **2011**, *45*, 9003−9008.